J. Korean Soc. Ind. Appl. Math. Vol.23, No.3, 203–210, 2019 http://doi.org/10.12941/jksiam.2019.23.203

THREE-DIMENSIONAL VOLUME RECONSTRUCTION BASED ON MODIFIED FRACTIONAL CAHN–HILLIARD EQUATION

YONGHO CHOI [1] AND SEUNGGYU LEE [2†]

[1]DEPARTMENT OF MATHEMATICS AND BIG DATA, DAEGU UNIVERSITY, GYEONGSAN-SI, GYEONGSANGBUK-DO 38453, REPUBLIC OF KOREA
Email address: yongho_choi@daegu.ac.kr

[2]DEPARTMENT OF MATHEMATICS AND RESEARCH INSTITUTE OF NATURAL SCIENCE, GYEONGSANG NATIONAL UNIVERSITY, JINJU 52828, REPUBLIC OF KOREA
Email address: sglee@gnu.ac.kr

ABSTRACT. We present the three-dimensional volume reconstruction model using the modified Cahn–Hilliard equation with a fractional Laplacian. From two-dimensional cross section images such as computed tomography, magnetic resonance imaging slice data, we suggest an algorithm to reconstruct three-dimensional volume surface. By using Laplacian operator with the fractional one, the dynamics is changed to the macroscopic limit of Levy process. We initialize between the two cross section with linear interpolation and then smooth and reconstruct the surface by solving modified Cahn–Hilliard equation. We perform various numerical experiments to compare with the previous research.

1. INTRODUCTION

Three-dimensional volume reconstruction has been various studied by using two-dimensional slice data such as computed tomography (CT) and magnetic resonance imaging (MRI). Using CT data, Vannier et al. implement complex craniofacial abnormalities reconstruction [1]. Koltai and Wood undertook a study of reconstruction from CT data, emphasizing the importance of three-dimensional reconstruction for accurate diagnosis in 1986 [2]. Marentette and Maise developed the list of conditions for which three-dimensional CT reconstruction such as acute complex trauma, posttumor reconstruction, delayed trauma reconstruction, and early trauma reconstruction [3]. Until recently, there have been various studies of 3D reconstruction using CT data: using dictionary learning [4], iterative reconstruction algorithm [5, 6], statistical analysis [7].

Received by the editors September 3 2019; Revised September 12 2019; Accepted in revised form September 14 2019; Published online September 25 2019.

2000 *Mathematics Subject Classification.* 65D18.

Key words and phrases. 3D volume reconstruction, fractional Cahn–Hilliard equation.

† Corresponding author.

The authors would like to thank Dr. Dongsun Lee for their helpful comments and suggestions.

Also there are various researches by using MRI data: brain tumor reconstruction from MRI with morphological operators and bicubic interpolation [8]. Gholipour et al. studied segmentation and volumetric reconstruction of fetal brain [9]. Yang et al. reconstruct mouse brain from histological sections with the guidance of MRI [10] and Lloyd et al. visualize the 3D fetal heart using prenatal MRI [11].

In particular, there was a previous study by Lee et al. [12], that research is three-dimensional volume reconstruction by using the modified Cahn–Hilliard (CH) equation from two planar cross sections. The difference between the work [12] and this paper is using the fractional CH equation to volume reconstruction. In recent years, the fractional CH equation has been studied [13, 14] and the image processing such as segmentation and inpaining is one of the most popular applications [15, 16].

In this paper, we show a effect of fractional CH equation to reconstruct the shapes from two parallel planes. A various simulations are conducted to compare the differences with the original CH equation.

We organize this paper as follow: in Section 2, we describe the reconstruction process from two parallel planes. In Section 3, explain a numerical solution and various simulation results are shown in Section 4. Finally, the conclusion is drawn in Section 5.

2. Reconstruction process

We use the following the CH equation with a fractional Laplacian for three-dimensional volume reconstruction:

$$\frac{\partial \phi(\mathbf{x},t)}{\partial t} = \Delta\left(F'(\phi(\mathbf{x},t)) + \epsilon^2\left(-\Delta\right)^s \phi(\mathbf{x},t)\right),\ \mathbf{x}\in\Omega,\ t>0, \tag{2.1}$$

where ϕ is the phase-field defined in $[-1,1]$, $F(\phi) = 0.25(1-\phi^4)$, ϵ is the coefficient related with the interacial energy, and $0 < s \leq 1$ is a fractional order. A surface of a reconstructed volume is represented by a zero-contour of ϕ. Note that the first Laplacian in the right hand side is related with the solution space H^{-1} of the gradient flow for deriving the CH equation from the Ginzburg–Landau free energy functional. Let ϕ_{top} and ϕ_{bottom} be respectively the top and bottom data on slices S_1 and S_2 (See Fig. 1).

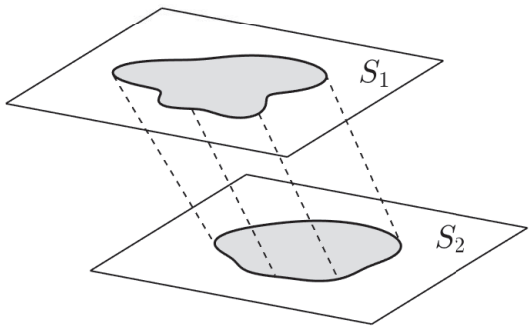

FIGURE 1. Schematic of slice data.

The initial condition is defined by the linear interpolation from ϕ_{top} and ϕ_{bottom} as follows:

$$\phi(x, y, \theta z_1 + (1-\theta)z_2) = \theta\phi_{top}(x, y) + (1-\theta)\phi_{bottom}(x, y),\ 0 \le \theta \le 1,$$

where z_1 and z_2 are the z-coordinate of the S_1 and S_2, respectively. Note that there is no fidelity term as a conventional reconstruction method. The term is replaced by a Dirichlet type boundary condition.

3. Numerical solution

We consider the Fourier spectral method in space and the linear convex splitting scheme in time [17]. The temporal discretization of (2.1) is firstly consider as follows:

$$\frac{\phi^{n+1} - \phi^n}{\Delta t} = \Delta\left((\phi^n)^3 - 3\phi^n + 2\phi^{n+1} + \epsilon^2(-\Delta)^s\phi^{n+1}\right). \tag{3.1}$$

For spatial discretization, we refer the spectral/Fourier definition of the fractional Laplacian [18]:

$$\mathcal{F}\left((-\Delta)^s\phi\right)(\xi) = |\xi|^{2s}\mathcal{F}(\phi)(\xi), \tag{3.2}$$

where $\mathcal{F}(\cdot)$ is a Fourier transformation with symbol $|\xi|^{2s}$. Since the drawback of this definition is valid only for a unbounded domain or a periodic boundary condition, we need to consider an additional strategy for a boundary condition, which will be discussed in later.

Applying the Fourier transform to (3.1) and using (3.2), the following discrete scheme can be derived:

$$\frac{\hat{\phi}^{n+1}_{pqr} - \hat{\phi}^n_{pqr}}{\Delta t} = -|\xi_{pqr}|^2\left(\left(\hat{\phi}^n_{pqr}\right)^3 - 3\hat{\phi}^n_{pqr} + 2\hat{\phi}^{n+1}_{pqr} + \epsilon^2|\xi_{pqr}|^{2s}\hat{\phi}^{n+1}_{pqr}\right),$$

where $\hat{\phi}^n_{pqr}$ is the discrete Fourier coefficient, $\xi_{pqr} = (2\pi p/L_x)^{2s} + (2\pi q/L_y)^{2s} + (2\pi r/L_x)^{2s}$, L_x, L_y, and L_z are respectively a length of a domain in x-, y-, and z-axis. The procedure stops when $\|\phi^{n+1} - \phi^n\|_\infty - \|\phi^n - \phi^{n-1}\|_\infty$ is less than a tolerance 10^{-12}. Instead of a fidelity term, the weighted average is used for the values of the top and bottom slices. Let N_{z_1} and N_{z_2} be positive integers such that $N_{z_1} = z_1/h$ and $N_{z_2} = z_2/h$. Then, the weighted average using α is calculated as follows:

$$\begin{aligned}
\phi^{n+1}_{ij,N_{z_1}} &= \alpha\phi^0_{ij,N_{z_1}} + (1-\alpha)\left(2\phi^{n+1}_{ij,N_{z_1}-1} - \phi^{n+1}_{ij,N_{z_1}-2}\right),\\
\phi^{n+1}_{ij,N_{z_2}} &= \alpha\phi^0_{ij,N_{z_2}} + (1-\alpha)\left(2\phi^{n+1}_{ij,N_{z_2}+1} - \phi^{n+1}_{ij,N_{z_2}+2}\right),
\end{aligned}$$

where $\alpha \in [0, 1]$. To deal with a bounded domain, we set $\phi^{n+1}_{ijk} = \phi^{n+1}_{ij,N_{z_1}}$ for $k = N_{z_1} + 1, \cdots, N_z$ and $\phi^{n+1}_{ijk} = \phi^{n+1}_{ij,N_{z_2}}$ for $k = 1, \cdots, N_{z_2} - 1$, i.e., there is dummy space to avoid the periodic boundary condition between the boundary of the computational domain and the slice data. Since the effect of α is already disscused in previous research [12], we use $\alpha = 0.5$ as in the research.

4. NUMERICAL SIMULATIONS

We perform numerical simulations to compare results with fractional and standard CH equation. Unless otherwise specified, we use the number of spatial grids $N = 64$, the spatial step size $h = 1/64$, the temporal step size $\Delta t = 0.1$, and $\epsilon = 4h/2\sqrt{2}\tanh^{-1}(0.9)$.

4.1. **Effect on reconstruction by height.** We first check the effect on the reconstruction by height. Let $N_h = N_{z_2} - N_{z_1}$ be the number of grid points depending on the reconstruction height. Figure 2 shows the reconstruction isosurface for the following oblique cylinder with different N_h:

$$\phi^0_{top} = \begin{cases} 1, & \sqrt{(x-0.6)^2+(y-0.5)^2} < 0.2 \\ -1, & \text{otherwise,} \end{cases}$$

$$\phi^0_{botton} = \begin{cases} 1, & \sqrt{(x-0.4)^2+(y-0.5)^2} < 0.2 \\ -1, & \text{otherwise.} \end{cases}$$

The reconstruction procedure fails in the case of Fig. 2 (b) since the height between slice data is too far. Based on the result, we use $N_h = 10$ unless otherwise specified.

(a) $N_h = 10$ (b) $N_h = 14$

FIGURE 2. Reconstruction isosurface for oblique cylinder with different N_h.

4.2. **Effect of fractional order s.** To check the fractional order s, we consider the oblique cylinder with the same initial condition in the previous simulation.

Figure 3 shows the reconstruction isosurface for a oblique cylinder with (a) $s = 0.25$, (b) $s = 0.5$, and (c) $s = 1$, which is a standard case. As seen in Figure 3 (a), the case $s = 0.25$, which is most small s, gives the artifical and awkward reconstruction result. Comparing with Figure 3 (b) and (c), we can notice that the former case gives more smooth isosurface result.

We also consider the standard cylinder with the following initial condition:

$$\phi^0_{top} = \phi^0_{botton} = \begin{cases} 1, & \sqrt{(x-0.5)^2+(y-0.5)^2} < 0.2 \\ -1, & \text{otherwise.} \end{cases}$$

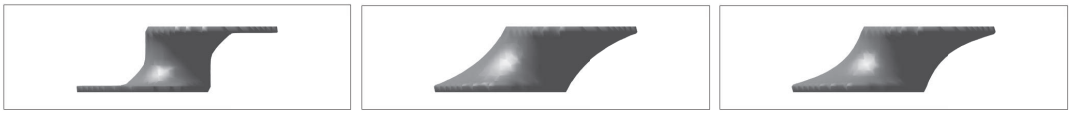

(a) $s = 0.25$ (b) $s = 0.5$ (c) $s = 1$

FIGURE 3. Reconstruction isosurface for oblique cylinder with different s.

Figure 4 shows the another reconstruction isosurface for a standard cylinder with same s valuse. Contrary to previous result, the case $s = 0.25$ gives the more reasonable reconsturction result than others.

(a) $s = 0.25$ (b) $s = 0.5$ (c) $s = 1$

FIGURE 4. Reconstruction isosurface for standard cylinder with different s.

The topology of the reconstruction is important since there are exmaples that cannot be processed when they violate the criterion by having intersection with a line perpendicular to the slices [19]. We consider the two cylinders with the following initial condition:

$$\phi^0_{top} = \phi^0_{botton} = \begin{cases} 1, & \sqrt{(x-0.38)^2 + (y-0.38)^2} < 0.15, \\ 1, & \sqrt{(x-0.62)^2 + (y-0.62)^2} < 0.15, \\ -1, & \text{otherwise.} \end{cases}$$

Figure 5 shows the reconstruction isosurface for two cylinders with different s. It is notable that the fractional order cases could prevent from changing topology (or emerging) even if the initial shape is quite close.

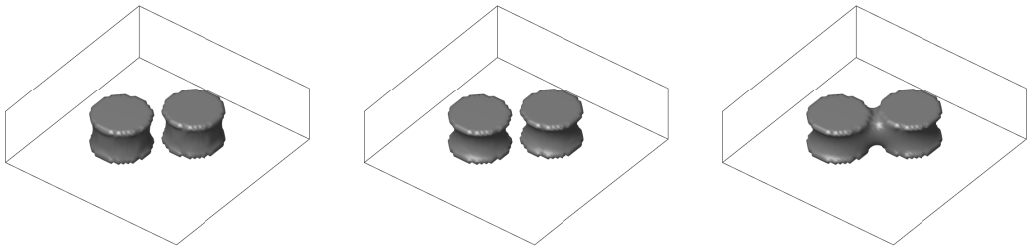

(a) $s = 0.25$ (b) $s = 0.5$ (c) $s = 1$

FIGURE 5. Reconstruction isosurface for two cylinders with different s.

4.3. **Various initial data.** We perform the reconsturction simulation with the following various initial data for top and bottom slice:

(a)

$$\phi^0_{top} = \begin{cases} 1, & \sqrt{(x-0.5)^2 + 0.5(y-0.5)^2} < 0.2, \\ -1, & \text{otherwise}, \end{cases}$$

$$\phi^0_{botton} = \begin{cases} 1, & \sqrt{0.5(x-0.5)^2 + (y-0.5)^2} < 0.2, \\ -1, & \text{otherwise}. \end{cases}$$

(b)

$$\phi^0_{top} = \begin{cases} 1, & \sqrt{(x-0.5)^2 + (y-0.5)^2} < 0.2, \\ -1, & \text{otherwise}, \end{cases}$$

$$\phi^0_{botton} = \begin{cases} 1, & (x,y) \in [0.2, 0.8] \times [0.2, 0.8], \\ -1, & \text{otherwise}. \end{cases}$$

(c)

$$\phi^0_{top} = \begin{cases} 1, & \sqrt{(x-0.3)^2 + 0.5(y-0.3)^2} < 0.15, \\ 1, & \sqrt{(x-0.7)^2 + 0.5(y-0.7)^2} < 0.15, \\ -1, & \text{otherwise}, \end{cases}$$

$$\phi^0_{botton} = \begin{cases} 1, & \sqrt{0.5(x-0.5)^2 + (y-0.5)^2} < 0.3, \\ -1, & \text{otherwise}. \end{cases}$$

(d)

$$\phi^0_{top} = \begin{cases} 1, & \sqrt{(x-0.3)^2 + 0.5(y-0.5)^2} < 0.12, \\ 1, & \sqrt{(x-0.7)^2 + 0.5(y-0.3)^2} < 0.12, \\ 1, & \sqrt{(x-0.7)^2 + 0.5(y-0.7)^2} < 0.12, \\ -1, & \text{otherwise}, \end{cases}$$

$$\phi^0_{botton} = \begin{cases} 1, & \sqrt{0.5(x-0.5)^2 + (y-0.5)^2} < 0.3, \\ -1, & \text{otherwise}. \end{cases}$$

Figure 6 shows contour of S_1 and S_2 (left) and reconstruction isosurfaces from the respective slice data (right). Each cases give different reconstruction results and it imply that the variable s value in space may gives better results when considering the practical use of our proposed algorithm such as multi-slice cross section.

5. CONCLUSIONS

We proposed the three-dimensional volume reconstruction model using the modified CH equation with a fractional Laplacian. The fractional order was expected to change the dynamics

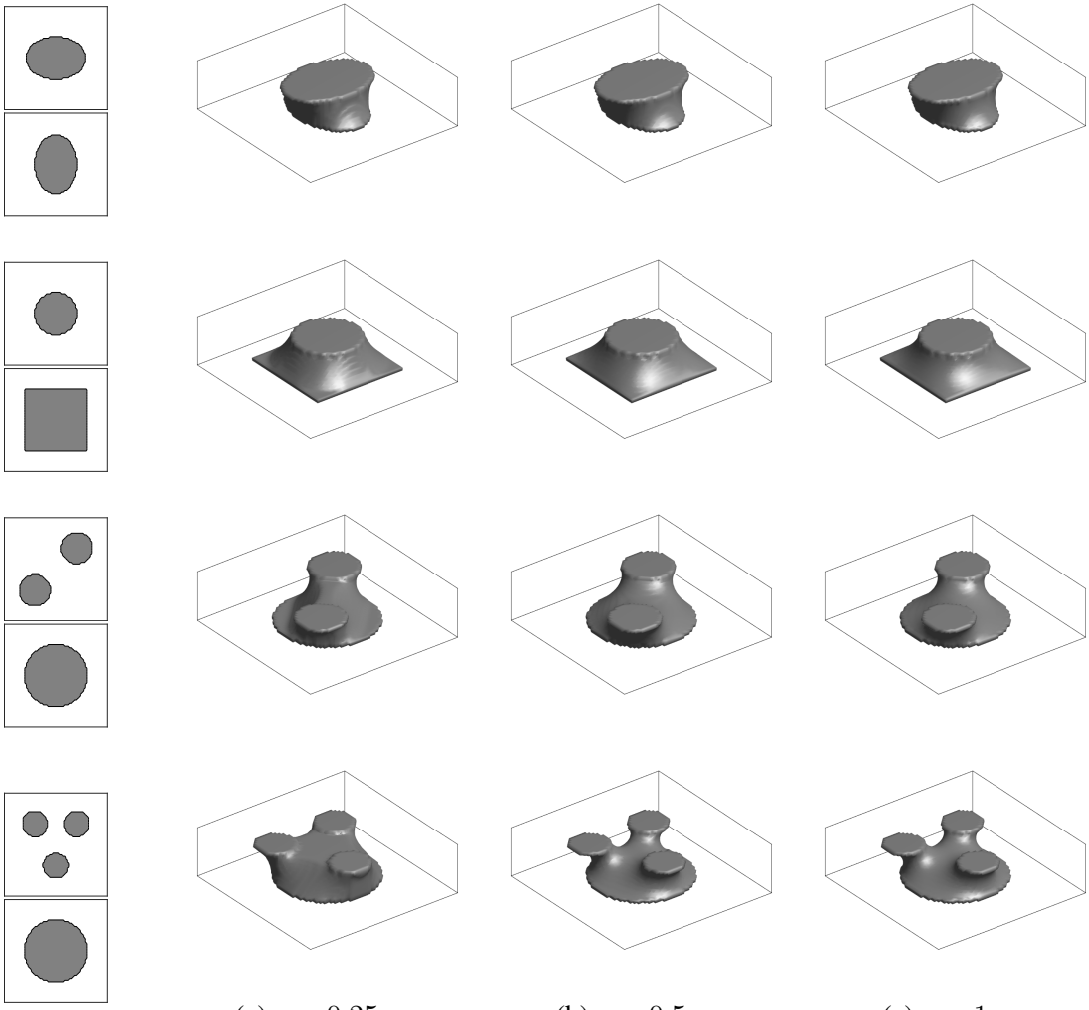

(a) $s = 0.25$ (b) $s = 0.5$ (c) $s = 1$

FIGURE 6. Contour of S_1 and S_2 (left) and reconstruction isosurfaces from respective slice data (right).

of the CH equation. We suggested a algorithm to reconstruct three-dimensional volume surface by using Laplacian operator with the fractional one. We initialized between the two parallel planes with linear interpolation and then smoothed and reconstructed the surface by solving modified CH equation. We performed various numerical simulations and compared the effect of fractional CH equation with original CH equation. It is observed that the reconstructed results are depending on the fractional order. In the future work, variable-order fractional Laplacian [20] would be discussed to more efficient reconstruction.

REFERENCES

[1] M.W. Vannier, J.L. Marsh, J.O. Warren, *Three dimensional CT reconstruction images for craniofacial surgical planning and evaluation*, Radiol., **150**(1) (1984), 179–184.

[2] P.J. Koltai and G.W. Wood, *Three dimensional CT reconstruction for the evaluation and surgical planning of facial fractures*, JAMA Otolaryngol. Head Neck Surg., **95**(1) (1986), 10–15.

[3] L.J. Marentette and R.H. Maise, *Three-dimensional CT reconstruction in midfacial surgery*, JAMA Otolaryngol. Head Neck Surg., **98**(1) (1988), 48–52.

[4] Z. Tian, X. Jia, K. Yuan, T. Pan, and S.B. Jiang, *Low-dose CT reconstruction via edge-preserving total variation regularization*, Phys. Med. Biol., **56**(18) (2011), 5949.

[5] A.K. Hara, R.G. Paden, A.C. Silva, J.L. Kujak, H.J. Lawder, and W. Pavlicek, *Iterative reconstruction technique for reducing body radiation dose at CT: feasibility study*, AJR Am. J Roentgenol., **193**(3) (2009), 764–771.

[6] L.L. Geyer, U.J. Schoepf, F.G. Meinel, J.W. Nance et al., *State of the art: iterative CT reconstruction techniques*, Radiol. **276**(2) (2015), 339–357.

[7] E. Soodmand, G. Zheng, W. Steens, R. Bader, L. Nolte, and D. Kluess, *Surgically Relevant Morphological Parameters of Proximal Human Femur: A Statistical Analysis Based on 3D Reconstruction of CT Data*, Orthop. Surg., **11**(1) (2019), 135–142.

[8] A. Amruta, A. Gole, and Y. Karunakar, *A systematic algorithm for 3-D reconstruction of MRI based brain tumors using morphological operators and bicubic interpolation*, 2010 2nd Int. Conf. Comp. Techn. Dev. IEEE, 2010.

[9] A. Gholipour, J.A. Estroff, C.E. Barnewolt, S.A. Connolly, and S.K. Warfield, *Fetal brain volumetry through MRI volumetric reconstruction and segmentation*, Int. J Comput. Assist. Radiol. Surg., **6**(3) (2011), 329–339.

[10] Z. Yang, K. Richards, N.D. Kurniawan, S. Petrou, and D.C. Reutens, *MRI-guided volume reconstruction of mouse brain from histological sections*, J Neurosci. Methods, **211**(2) (2012), 210–217.

[11] D.F.A. Lloyd, K. Pushparajah, J.M. Simpson, J.F.P. van Amerom, M.P.M van Poppel et al., *Three-dimensional visualisation of the fetal heart using prenatal MRI with motion-corrected slice-volume registration: a prospective, single-centre cohort study*, The Lancet, **393**(10181) (2019), 1619–1627.

[12] S. Lee, Y. Choi, D. Lee, H.K. Jo, S. Lee, S. Myung, and J. Kim, *A modified Cahn–Hilliard equation for 3D volume reconstruction from two planar cross sections*, J. Korean Soc. Ind. Appl. Math., **19**(1) (2015), 47–56.

[13] M. Ainsworth and Z. Mao, *Analysis and approximation of a fractional Cahn–Hilliard equation*, SIAM J. Numer. Anal., **55**(4) (2017) 1689–1718.

[14] Z. Weng, S. Zhai, and X. Feng, *A Fourier spectral method for fractional-in-space Cahn—Hilliard equation*, Appl. Math. Model., **42** (2017) 462–477.

[15] J. Bosch and M. Stoll, *A fractional inpainting model based on the vector-valued Cahn–Hilliard equation*, SIAM J. Imaging Sci., **8**(4) (2015) 2352–2382.

[16] D. Lee and S. Lee, *Image segmentation based on modified fractional Allen–Cahn equation*, Math. Probl. Eng., **2019** (2019) 3980181.

[17] D. Eyre, *Unconditionally gradient stable time marching the Cahn–Hilliard equation*, MRS Proc., **529** (1998) 39.

[18] A. Lischke, G. Pang, M. Gulian, F. Song, C. Glusa, X. Zheng, W. Cai, M. Meerschaert, M. Ainsworth, and G. Karniadakis, *What is the fractional Laplacian?*, arXiv preprint arXiv:1801.09767 (2018).

[19] C. Bajaj, E. Coyle, and K. Lin, *Arbitrary topology shape reconstruction from planar cross sections*, Graph. Model. Im. Proc., **58**(6) (1996) 524–543.

[20] M. Xiang, B. Zhang, and D. Yang, *Multiplicity results for variable-order fractional Laplacian equations with variable growth*, Nonlinear Anal. **178** (2019) 190–204.